


# Pilot Study of Endovascular Delivery of Mesenchymal Stromal Cells in the Aortic Wall in a Pig Model

Cell Transplantation  
Volume 30: 1–7  
© The Author(s) 2021  
Article reuse guidelines:  
sagepub.com/journals-permissions  
DOI: 10.1177/09636897211010652  
journals.sagepub.com/home/ctl  


Ke Li<sup>1</sup>, Deborah Vela<sup>2</sup>, Elton Migliati<sup>1</sup>, Maria da Graca Cabreira<sup>1</sup>, Xiaohong Wang<sup>1</sup>, L Maximilian Buja<sup>2,3</sup>, and Emerson C. Perin<sup>1</sup> 

## Abstract

Abdominal aortic aneurysms (AAAs) have a high mortality. In small-animal models, multipotent mesenchymal stromal cells (MSCs) have shown benefits in attenuating aneurysm formation. However, an optimal cell delivery strategy is lacking. The NOGA system, which targets cell injections in a less-invasive way, has been used for myocardial cell delivery. Here, we assessed the safety and feasibility of the NOGA system for endovascular delivery of MSCs to the aortic wall in an AAA pig model. We induced AAA in 9 pigs by surgery or catheter induction. MSCs were delivered using the NOGA system 6 or 8 weeks after aneurysm induction. We euthanized the pigs and harvested the aorta for histologic analysis 1, 3, and 7 days after cell delivery. During AAA creation, 1 pig died; 8 pigs completed the study without acute adverse events or complications. The cell delivery procedure was safe and feasible. We successfully injected MSCs directly into the aortic wall in a targeted manner. Histologic and immunohistochemical analyses confirmed transmural injections in the aortic wall area of interest and the presence of MSCs. Our study showed the safety and feasibility of endovascular cell delivery to the aortic wall in a pig model.

## Keywords

cardiovascular diseases, vascular diseases, abdominal aortic aneurysm, cell transplantation, mesenchymal stromal cells

## Introduction

No therapies are currently available to effectively prevent abdominal aortic aneurysm (AAA) dilation. Significant interest has developed in identifying ways to prevent AAA expansion and reduce the risk of rupture. Multipotent mesenchymal stem cells (MSCs) have shown benefits in attenuating aneurysm formation<sup>1,2</sup> in animal AAA models, and a clinical trial is underway to examine the effects of MSCs on aneurysm growth in patients with small AAAs<sup>3</sup>.

The most common route of cell delivery is intravenous injection, which often leads to trapping of cells in other organs<sup>4,5</sup>. Directly injecting MSCs into the aortic wall by exposing the infrarenal aorta<sup>6</sup>, although allowing a targeted delivery, is highly invasive; therefore, a less-invasive, more targeted cell delivery strategy is needed.

The NOGA system has been widely used to deliver cells into endomyocardial tissues and has been safe and efficacious<sup>7,8</sup>. This approach allows the operator to reconstruct a 3D map that can be used to perform specifically targeted injections. As a catheter-based system, it requires only percutaneous arterial access. Here, we examined the

safety and feasibility of using the NOGA system for endovascular cell delivery in the pig aorta.

## Materials and Methods

All procedures in the domestic pigs used in this study were conducted under general anesthesia and were approved by the Texas Heart Institute's Institutional Animal Care and Use committee.

<sup>1</sup> Stem Cell Center, Texas Heart Institute, Houston, Texas, USA

<sup>2</sup> Cardiovascular Pathology, Texas Heart Institute, Houston, Texas, USA

<sup>3</sup> Department of Pathology and Laboratory Medicine, The University of Texas Health Science Center at Houston McGovern Medical School, Houston, Texas, USA

Submitted: July 1, 2019. Revised: March 30, 2021. Accepted: March 30, 2021.

### Corresponding Author:

Emerson C. Perin, MD, PhD, Stem Cell Center, Texas Heart Institute, 6770 Bertner Avenue, MC 2-255, Houston, Texas 77030, USA.  
Email: eperin@texasheart.org



### **Animal Model**

We used 9 domestic pigs (6 males, 3 females). We induced aneurysm formation surgically in 1 pig; in 8 pigs, we used an intraluminal catheter-based approach to chemically induce aneurysm formation. One pig in the catheter-based group died 1 day after aneurysm. Briefly, on day 0, we induced aneurysm formation, and MSCs were delivered 6 or 8 weeks later; this time point was chosen to avoid the intense focal inflammatory response period and to allow dilation to occur. Eight pigs were included in the data analysis. At 1, 3, or 7 days after cell delivery, we humanely euthanized the pigs according to the American Veterinary Medical Association Guidelines on Euthanasia<sup>9</sup>.

### **AAA Creation**

For surgical aneurysm induction ( $n = 1$ ), the aorta was exposed via a dorsal recumbency laparotomy and dissection of the infrarenal abdominal aorta. After positioning vascular clamps caudal to the renal arteries and cranial to the iliac arteries in the aorta, we injected a solution of collagenase (8000 units, Worthington Biochemical Corporation, Lakewood, NJ, USA) and elastase (30 units, Sigma-Aldrich, St. Louis, MO, USA) in the aortic lumen for 15 minutes. The aorta was washed with isotonic saline, and the abdominal cavity was closed in standard fashion.

In all other pigs, we used a catheter-based endovascular chemical induction of aneurysm by administering calcium chloride (25%) as described<sup>10</sup> (Supplemental Table 1). The pigs were prepped for sterile access to the inguinal area. We gained femoral access via bilateral percutaneous punctures with an 8Fr introducer sheath. A triple-lumen catheter was inserted in the femoral vein in case a rapid infusion of high-volume solutions was needed. To prevent clotting, we administered 5,000-10,000 IU of unfractionated heparin. A marker pigtail catheter was advanced retrograde through the descending aorta to just proximal to the renal artery for performing angiography. Two noncompliant angioplasty balloons (9-, 10-, or 11-mm in diameter based on angiographic measurements) were positioned immediately over the adjacent vertebral arteries and inflated simultaneously to occlude aortic flow. We confirmed successful aortic occlusion by measuring femoral arterial blood pressure and performing angiography. We then infused calcium chloride, washed the remaining solution from the aortic lumen, and removed the catheters.

### **MSC Preparation**

Bone marrow was harvested from the iliac crest of a juvenile pig. Mononuclear cells (MNCs) were isolated from the bone marrow by Ficoll density-gradient centrifugation (GE Healthcare Life Sciences, Marlborough, MA, USA). MNCs were plated at  $2.5 \times 10^5$  cell/cm<sup>2</sup> in growth medium (Alpha modified Minimum Essential Medium supplemented with

10% fetal bovine serum) for MSC isolation. After noting adherent colonies at 10 days, we started the cell expansion process. Cells were plated at a density equivalent to 500 cells/cm<sup>2</sup>. Expansion comprised two passages of cell plating at 500 cells/cm<sup>2</sup>. During the second passage, cells were transduced with a pLVXacGFP lentiviral preparation (Clontech Laboratories, Inc., Fremont, CA, USA) as described by the supplier. To select GFP-expressing cells, we sorted the cells by flow cytometry (BD-FACSaria, BD Biosciences, San Jose, CA, USA) 5-7 days after transduction. GFP cells were subjected to expansion by passage 3 as described earlier. Semi-confluent cultures were then cryopreserved. Cells were thawed as needed and subjected to a fourth expansion round. For NOGA injections, the MSCs were collected and suspended in phosphate-buffered saline (concentration of  $33.4 \times 10^6$  cells/ml).

### **Endovascular Mapping and Cell Delivery**

We used the NOGA platform (Biosense Webster, Diamond Bar, CA, USA) for cell delivery. The system comprises a triangular location pad to generate ultralow magnetic field energy, a stationary reference patch with a miniature magnetic field sensor, and a workstation for information processing and 3-D reconstruction. The left femoral artery was exposed through a femoral percutaneous puncture, and an 8F sheath was inserted. We performed an angiogram of the aorta at the aneurysm site to obtain anatomical references. Then, a MYOSTAR injection catheter (Biosense Webster) connected to the NOGA system was advanced to the aortic area of interest. Using the electrode on the injection catheter, we acquired a series of points in the aortic intima and recorded the information to construct an aortic map. MSCs (concentration of  $33.4 \times 10^6$  cells/ml) were injected into the aortic wall in a 0.2-mL volume/injection in a site cranial or caudal to the aneurysm. We performed 10-20 60-second injections per pig. Then, we removed the catheter and repaired the artery. The pigs were transferred to the intensive care unit for monitoring. Before the first procedure, we performed a small angiographic pilot study, with the use of dye and contrast, to identify the optimal needle length for injection depth (2 mm).

### **Tissue Harvest and Histologic Evaluation**

For euthanasia, the pigs were placed under a deep plane of surgical anesthesia and given adequate anticoagulation; the heart was arrested using an injection of 20–90 mEq of KCL. The aortic segment of interest was dissected and harvested. We excised the abdominal aorta 2-3 cm above the renal arteries and 2-3 cm below the iliac arteries. The sample was photographed, radiographed, and fixed in 10% neutral buffered formalin for 24–48 hours. The aortic sample was sliced open along its ventral or dorsal face and sectioned into approximately 2-mm cross-sectional rings. All tissues were processed for paraffin embedding. Histologic sections were stained with hematoxylin and eosin, and sections from selected rings were stained with

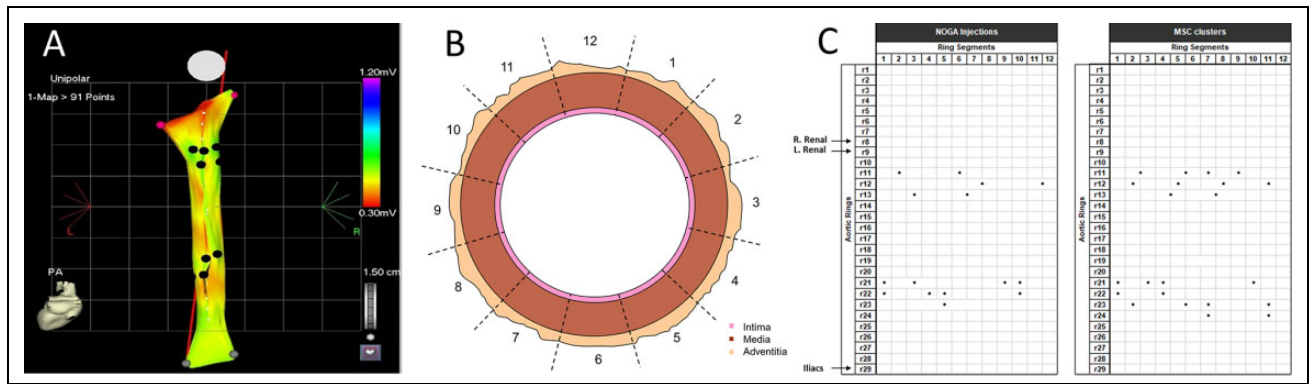


**Figure 1.** NOGA mapping of the infrarenal aorta. (A) Posterior-anterior (PA) view of the respective NOGA map and injection results. Pink dots, left and right renal arteries; gray dots, left and right iliac arteries; black dots, injection sites, distributed as 2 groups corresponding to the cranial and caudal edges of the aneurysm. (B) Diagram of the aorta divided into 12 areas to facilitate correlation with NOGA mapping. (C) The grids show the plotted histopathologic findings corresponding to needle tracks (left) and MSC cluster locations (right). The NOGA map shows that the cranial set of injections were delivered closer to the ostia of the renal arteries than were the caudal injections delivered relative to the ostia of the iliac arteries. This asymmetry is also reflected in the injury sites plotted in the histologic evaluation chart.

Masson's trichrome, Verhoeff-Van Gieson, and anti-GFP antibody (Abcam, Cambridge, MA, USA #6556). We assessed acute or chronic changes in the aortic wall and confirmed the presence of injected MSCs by histologic evaluation.

### Correlation with NOGA Mapping

For spatial orientation and consistency in reporting the location of specific histopathologic features or findings, we divided the circumference of the aortic rings into 12 areas (30° each) that were labeled numerically in clockwise fashion. This approach generated a chart or grid that could be roughly correlated with the injection maps produced by the NOGA system. The site where the aorta had been cut open for gross inspection corresponded to region 6 or 12 (Fig. 1B). CAAS software (Cardiovascular Angiography Analysis System 5.4, Pie Medical Imaging, Maastricht, Netherlands) was used for angiography measurements.

### Statistical Analysis

All values were expressed as mean + standard deviation. To compare continuous variables, we used an unpaired Student t test;  $P < .05$  was considered significant. Correlations between aortic segment lengths measured by NOGA and angiography were calculated, and the Pearson correlation index was reported. A Bland-Altman analysis was used to compare aortic length measurements obtained by NOGA and angiography (computed as the difference [NOGA-angiography] versus the average [NOGA, angiography]).

## Results

### Pig Aortic Aneurysm Model

Aneurysm creation was inconsistent in our model. At postoperative day (POD) 21, only 2 (both from the

catheter-induced group) of the 8 pigs in the study showed angiographic signs of focal dilatation in the infrarenal aorta. Histopathologic examination confirmed successful aortic aneurysm creation only in these 2 pigs; the affected portion of the aorta presented as a mild bulge or area of dilation with wall thinning characterized by focal or diffuse hardening. Radiographic imaging confirmed dilatation of the lumen and calcification. On microscopic examination, the thinned aortic wall showed changes in architecture. The internal elastic lamina and elastin fibers of the medial lamellar units, although generally preserved, were somewhat attenuated and appeared flat, without the typical fenestrated appearance (Supplemental Fig. 1). In addition, we noted a paucity of nuclei and marked smooth muscle cell loss, making the lamellar units appear thinner and collapsed; the interstitium was characterized by mineralized extracellular matrix. Calcification often extended into the adventitia, with chronic inflammation and scarce multinucleated giant cells at the outer margin. Mild intimal proliferation was usually present in the overlying intimal layer.

A third pig showed some areas of focal wall thinning and calcification in the distal portion of the infrarenal aortic segment but failed to develop aneurysmal dilation. We also saw two sites of healed focal transmural injury, attributed to excessive focal pooling of the agent used for aneurysm induction.

The other 5 pigs without aneurysm formation showed chronic mural changes such as focal or multifocal areas of neointimal formation or medial fibrosis, with mild wall thickening. These findings were attributed to mural injury produced during lesion creation.

### Endovascular Mapping and Cell Delivery

We successfully performed mapping and injections in 8 pigs, with 100% survival. No complications (eg, aortic rupture, bleeding, or sudden death) occurred during the procedures.

The abdominal aortic lumen provided easy accessibility for manipulating the injection catheter. Blood flow did not interfere with moving or positioning the catheter. Using the abdominal aortic angiogram as a reference, we easily identified anatomic landmarks (eg, renal and iliac arteries) and set them as boundaries for our target mapping segment. The entire intimal surface of the infrarenal aortic segment was accessed by the catheter without difficulty, and 3-D maps were promptly generated using the NOGA system (Fig. 1A).

To verify the anatomic accuracy of NOGA mapping, we compared the measured length of aortic segments obtained from the NOGA system to that seen on angiogram in 7 pigs (Supplemental Table 2). We found a strong correlation between the 2 measurements ( $r = .99$ ,  $P < .0001$ ; Supplemental Fig. 2A). Bland-Altman analysis showed that measurements obtained using NOGA mapping were slightly larger than those obtained on angiography, with a mean difference of 5.7 mm; the 95% limit of agreement ranged from -1.5 mm to 12.99 mm (Supplemental Fig. 2B). During mapping, we also collected tissue voltage information using the NOGA system. We compared the average unipolar voltage between supra-renal and infrarenal (aneurysm target) aortic tissue and found no significant difference between the regions (normal tissue:  $0.61 \pm 0.18$  mv versus aneurysm target tissue:  $0.62 \pm 0.17$  mv,  $P = .96$ ; Supplemental Table 3).

After generating the NOGA map, we successfully identified the cranial and caudal regions of the infrarenal aorta (presumed to border the proximal and distal edges of the aneurysm) and performed 10-20 transmural MSC injections in normal tissue in the target area; the injections were equally distributed between the cranial and caudal sites. The total number of injection sites was 108 in 8 pigs; no acute adverse effects were noted. The injection sites were plotted in each respective NOGA map and were compared with the findings plotted in histologic analysis charts. Overall, the anatomical localization of the NOGA injections correlated well with the histologic analysis (Fig. 1C). However, we were not able to obtain the exact number of NOGA injections in the histologic analysis due mainly to the 2-mm sampling interval and the occasional merging and dissemination of the MSC injection boluses into the adventitia. No instances of aortic perforation were noted on angiographic or histologic examination.

### Endovascular Cell Delivery Safety

All infrarenal aortic segments showed evidence of NOGA injections. On macroscopic examination, the luminal surface of the aorta had small pinpoint or short linear puncture-like wounds that were roughly 1-mm wide and were occasionally surrounded by mild hemorrhage (Fig. 2A-C). The injuries appeared relatively more traumatic at some injection sites, presenting as larger coalescing areas of subintimal hemorrhage or more obvious disruption to the vessel wall. All luminal lesions tended to be grouped at 2 main locations:

distal to the renal artery ostia and proximal to the iliac artery ostia. The lesions closely matched the distribution of injection sites displayed in the respective NOGA maps (Fig. 1A-C). The adventitial side of the vessel contained small areas of hemorrhage at locations closely matching the needle entrance wounds on the luminal side of the wall. These adventitial hemorrhages presented as small hematomas or in diffuse patterns.

Microscopically, the needle entrance wounds consisted mostly of a small linear tear, perpendicular to the intimal surface; the depth of the tear varied, ranging from a superficial tear that compromised only the intimal layer to a fully transmural tear that reached the adventitia (Fig. 2D-F). Some pigs showed increased numbers of very superficial perpendicular tears that were not always associated with adventitial hemorrhage (generally indicative of successful transmural penetration). In other instances, the mural tears also extended transversely or longitudinally within the media. Both perpendicular and transverse tears were often accompanied by varying degrees of hemorrhage. In 2 pigs, we noted more significant focal transverse tears with greater hemorrhage that formed small intramural hematomas in some areas, possibly due to intramedial delivery of the MSC injection bolus or needle slippage (Supplemental Fig. 3).

By 7 days after NOGA injections, the needle entrance wounds showed signs of active healing. The perpendicular puncture wounds were still noticeable on gross inspection, but with little to no hemorrhage. Microscopically, the lesions showed signs of endothelialization; however, the defect in the aortic wall remained without signs of closure. The larger transverse intramedial tears showed signs of residual hemorrhage and were surrounded by a margin or halo of smooth muscle loss and extracellular matrix deposition.

Most of the NOGA needle injury sites were found in areas of otherwise normal aorta; however, occasionally, injections were delivered to areas of wall thinning and/or calcification.

### MSC Delivery and Retention

In pigs euthanized 1 or 3 days after NOGA injections, immunohistochemical staining confirmed the presence of MSCs at the injection sites. Cells were mostly seen in the adventitial and periadventitial regions, as part of larger accumulations or clusters within areas of hemorrhage or microhematomas that were observed macroscopically or as groups of smaller cell aggregates disseminated within the adventitial connective tissue (Supplemental Figs. 4 and 5). Occasionally, MSCs were observed within the layers of the media. In small interstitial infiltrates, the cells appeared mostly viable. However, in the larger accumulations, the cluster core tended to show signs of cell degeneration or necrosis and acute inflammatory cell infiltration mixed with variable amounts of blood.

In pigs euthanized at 7 days after cell injections, no GFP+ areas were observed in the adventitia or media. The adventitial microhematomas showed signs of active

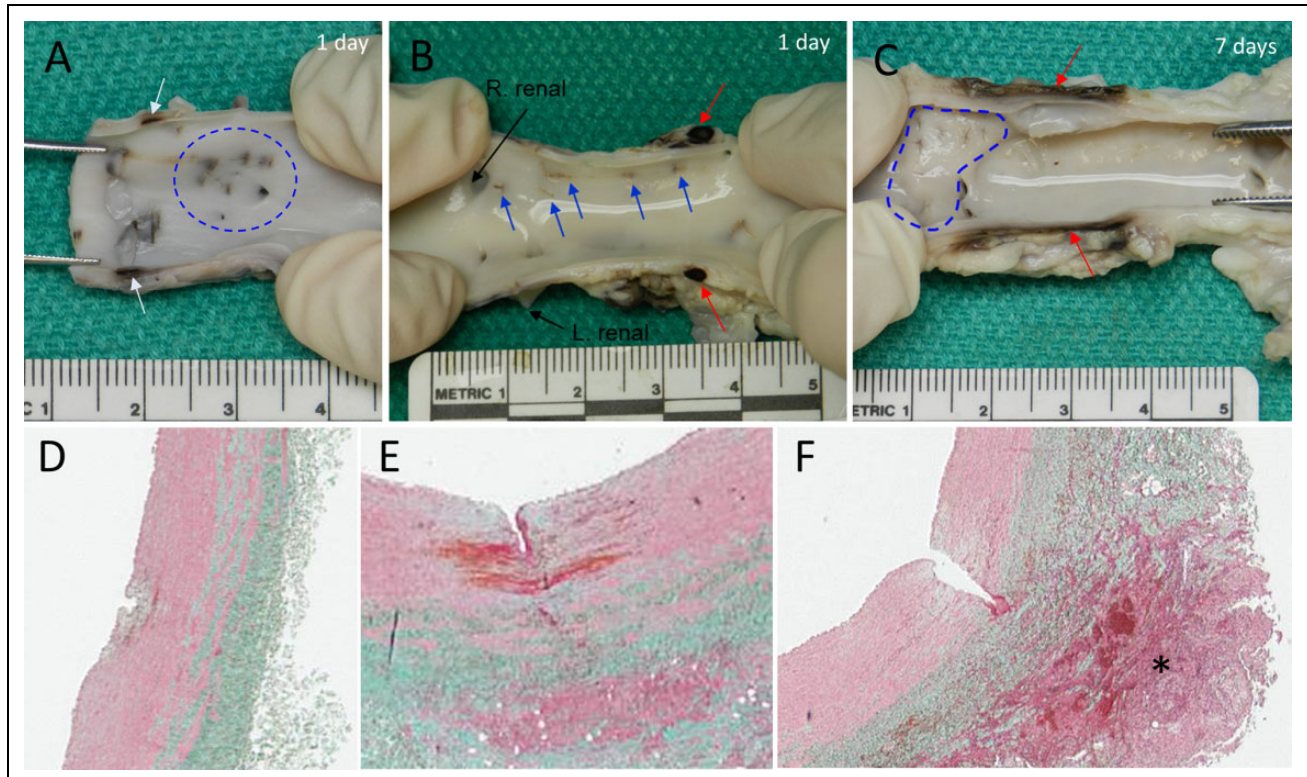


**Figure 2.** Gross and histologic appearance of NOGA needle entrance wounds. (A) Cluster of small puncture-like wounds (dotted circle) and small intramural hemorrhages (white arrows) 2 cm proximal to the iliac artery ostia. (B) Group of linear intimal breaches (blue arrows), connected by mild "scratches" on the intimal surface, and a small adventitial microhematoma (red arrows) located below the renal artery ostia. (C) By 7 days after cell injections, the mild focal hemorrhage was mostly cleared from the puncture-like entrance wounds (dotted outline), but diffuse residual periadventitial hemorrhage (red arrows) was still present. Injection injury patterns of NOGA needle entrance wounds (D-F, Masson's trichrome stain.). Most entrance wounds presented as perpendicular tears ranging from superficial (D), mid (E), to transmural depths with adventitial microhematomas (F, asterisk).

healing, mild chronic inflammation, and incipient extracellular matrix deposition.

## Discussion

This is the first study, to our knowledge, in which the NOGA platform has been used to deliver MSCs by the endovascular route in the abdominal aorta. Our results showed anatomical accuracy of the NOGA maps generated for the infrarenal aorta when compared to angiography, and we were able to delineate the 3D intima surface of the aorta. The injection catheter we used has a retractable needle in the tip, which allows the operator to adjust the needle's length per tissue depth. During cell delivery, aortic blood flow was stable, and no perforations or complications occurred. The histologic and immunohistochemical analyses confirmed the presence of cells mostly in targeted area. Our findings show that the NOGA system may be a less invasive, more targeted cell delivery strategy for the aorta.

The NOGA platform was originally designed to deliver cells directly into the myocardium through transendocardial injections<sup>11</sup> and has been safe and efficacious<sup>7,8</sup>. Our safety and feasibility results in this study support those our group

has found using the NOGA system for transendocardial delivery of cells to the heart<sup>8,12</sup>. However, in this pilot study, we discovered that adapting the NOGA system for aortic wall injections may not be straightforward. First, the catheter was designed for use in the heart chamber; affixing the needle at a strict perpendicular orientation for deploying inside the aortic lumen, which is much narrower than the heart, was challenging. Thus, the needle tracks tended to be somewhat slanted, which led to scratches upon needle deployment and caused minimal or very superficial perpendicular tears. Second, the aortic wall is much thinner than the myocardium, and the 27G needle and the 0.2-ml volume may be too big for use in the aorta. Many local small hematomas and some areas of extensive mural trauma were seen on histologic examination. We need to consider the possibility the needle may penetrate the aortic wall in some scenarios, as seen in our study. However, we did not observe any catastrophic hemorrhagic events, but a smaller needle may minimize the risk. Therefore, a catheter comprising an acute angle and a smaller-gauge needle may be needed for aortic-specific injections. Moreover, injection-related injuries could have long-term negative effects, such as an inflammatory response that may weaken the wall or destroy delivered cells.

Although we monitored the pigs for up to 7 days after cell injections, our histologic studies showed signs of active healing in many wounds; therefore, we cannot clearly determine the long-term effects at this stage. Studies with longer periods of observation are needed.

The NOGA system can collect electrophysiological information during mapping and injection. In myocardium mapping, ischemic areas have significantly lower unipolar voltage than normal areas. In aortic mapping in the present study, no voltage difference was observed between aneurysm-related areas and normal tissue. The 10-fold difference in thickness between the aortic wall and the myocardium may be one reason that we observed a 10-fold difference in the average unipolar voltage (0.6 mv in the aortic wall versus >7 mv in the myocardium), meaning the unipolar voltage in the aorta wall is too low to detect the difference. Another reason may be the low incidence and degree of aneurysmal changes that we produced in our animal model. Nonsignificant pathological changes may not induce a significant change in unipolar voltage, making the voltage difference too small to be detected in the aorta. Thus, identifying the aneurysmal area in the aorta may require adding fluoroscopy imaging to the NOGA approach to locate anatomic landmarks, whereas in myocardium mapping, the NOGA system alone can accurately identify ischemic areas.

The main limitation of our study is the failure of the AAA model. However, because targeted injections were made in normal tissue, we believe this failure did not significantly affect the safety and feasibility aspects of the injections.

In conclusion, we demonstrated the successful targeted delivery of MSCs to the aortic wall using the NOGA system, with no acute complications. However, the system may need to be modified for use in the aorta to decrease injection-associated injuries, and longer monitoring periods may be required. Our findings provide a basis for further study of this less-invasive approach for delivering cell therapy or other drugs for AAA treatment.

### Acknowledgments

The authors thank Rebecca A. Bartow, PhD, of the Texas Heart Institute, for editorial support.

### Ethical Approval

Ethical approval to report this study was obtained from the Texas Heart Institute's Institutional Animal Care and Use Committee (Protocol ID:2013-20 and 2015-03).

### Statement of Human and Animal Rights

All procedures in this study involving animals were conducted in accordance with the Texas Heart Institute's Institutional Animal Care and Use Committee-approved protocols (Protocol ID:2013-20 and 2015-03).

### Statement of Informed Consent

There are no human subjects in this article; informed consent is not applicable.


### Declaration of Conflicting Interests

The author(s) declared no potential conflicts of interest with respect to the research, authorship, and/or publication of this article.

### Funding

The author(s) disclosed receipt of the following financial support for the research, authorship, and/or publication of this article: Dr. Emerson C. Perin was supported in part by the McNair Scholars Program at the Texas Heart Institute.

### ORCID iD

Emerson C. Perin  <https://orcid.org/0000-0002-3622-9814>

### Supplemental Material

Supplemental material for this article is available online.

### References

1. Hashizume R, Yamawaki-Ogata A, Ueda Y, Wagner WR, Narita Y. Mesenchymal stem cells attenuate angiotensin II-induced aortic aneurysm growth in apolipoprotein E-deficient mice. *J Vasc Surg.* 2011;54(6):1743–1752.
2. Sharma AK, Lu G, Jester A, Johnston WF, Zhao Y, Hajzus VA, Saadatzadeh MR, Su G, Bhamidipati CM, Mehta GS, Kron IL, et al. Experimental abdominal aortic aneurysm formation is mediated by IL-17 and attenuated by mesenchymal stem cell treatment. *Circulation.* 2012;126(11 Suppl 1):S38–S45.
3. Wang SK, Green LA, Gutwein AR, Drucker NA, Motagana-halli RL, Fajardo A, Babbey CM, Murphy MP. Rationale and design of the ARREST trial investigating mesenchymal stem cells in the treatment of small abdominal aortic aneurysm. *Ann Vasc Surg.* 2018;47:230–237.
4. Fu XM, Yamawaki-Ogata A, Oshima H, Ueda Y, Usui A, Narita Y. Intravenous administration of mesenchymal stem cells prevents angiotensin II-induced aortic aneurysm formation in apolipoprotein e-deficient mouse. *J Transl Med.* 2013;11:175.
5. Yamawaki-Ogata A, Hashizume R, Fu XM, Usui A, Narita Y. Mesenchymal stem cells for treatment of aortic aneurysms. *World J Stem Cells.* 2014;6(3):278–287.
6. Turnbull IC, Hadri L, Rapti K, Sadek M, Liang L, Shin HJ, Costa KD, Marin ML, Hajjar RJ, Faries PL. Aortic implantation of mesenchymal stem cells after aneurysm injury in a porcine model. *J Surg Res.* 2011;170(1):e179–e188.
7. Perin EC, Tian M, Marini FC 3rd, Silva GV, Zheng Y, Baimbridge F, Quan X, Fernandes MR, Gahremanpour A, Young D, Paolillo V, et al. Imaging long-term fate of intramyocardially implanted mesenchymal stem cells in a porcine myocardial infarction model. *PLoS One.* 2011;6(9):e22949.
8. Zheng Y, Sampaio LC, Li K, Silva GV, Cabreira-Hansen M, Vela D, Segura AM, Bove C, Perin EC. Safety and feasibility of mapping and stem cell delivery in the presence of an implanted left ventricular assist device: a preclinical investigation in sheep. *Tex Heart Inst J.* 2013;40(3):229–234.
9. American Veterinary Medical Association. AVMA Guidelines for the Euthanasia of Animals: 2013 Edition. Accessed May 1, 2018. <https://www.avma.org/KB/Policies/Documents/euthanasia.pdf>.

10. Klink A, Hyafil F, Rudd J, Faries P, Fuster V, Mallat Z, Meilhac O, Mulder WJ, Michel JB, Ramirez F, Storm G, et al. Diagnostic and therapeutic strategies for small abdominal aortic aneurysms. *Nat Rev Cardiol.* 2011;8(6):338–347.
11. Psaltis PJ, Zannettino AC, Gronthos S, Worthley SG. Intra-myocardial navigation and mapping for stem cell delivery. *J Cardiovasc Transl Res.* 2010;3(2):135–146.
12. Perin EC, Silva GV, Henry TD, Cabreira-Hansen MG, Moore WH, Coulter SA, Herlihy JP, Fernandes MR, Cheong BY, Flamm SD, Traverse JH, et al. A randomized study of transendocardial injection of autologous bone marrow mononuclear cells and cell function analysis in ischemic heart failure (FOCUS-HF). *Am Heart J.* 2011;161(6):1078–1087 e1073.